Permanent reduction of dissipation in nanomechanical Si resonators by chemical surface protection

Y Tao[1,2], P Navaretti[1,3], R Hauert[4], U Grob[1], M Poggio[3] and C L Degen[1]

[1] Department of Physics, ETH Zurich, Otto Stern Weg 1, 8093 Zurich, Switzerland
[2] Department of Chemistry, Massachusetts Institute of Technology, 77 Massachusetts Avenue, Cambridge MA 02139, USA
[3] Department of Physics, University of Basel, Klingelbergstrasse 82, 4056 Basel, Switzerland
[4] Empa, Swiss Federal Laboratories of Materials Science and Technology, Überlandstrasse 129, 8600 Dübendorf, Switzerland

E-mail: degenc@ethz.ch

CrossMark

Abstract

We report on mechanical dissipation measurements carried out on thin ($\sim$100 nm), single-crystal silicon cantilevers with varying chemical surface termination. We find that the 1–2 nm-thick native oxide layer of silicon contributes about 85% to the friction of the mechanical resonance. We show that the mechanical friction is proportional to the thickness of the oxide layer and that it crucially depends on oxide formation conditions. We further demonstrate that chemical surface protection by nitridation, liquid-phase hydrosilylation, or gas-phase hydrosilylation can inhibit rapid oxide formation in air and results in a permanent improvement of the mechanical quality factor between three- and five-fold. This improvement extends to cryogenic temperatures. Presented recipes can be directly integrated with standard cleanroom processes and may be especially beneficial for ultrasensitive nanomechanical force- and mass sensors, including silicon cantilevers, membranes, or nanowires.

S Online supplementary data available from stacks.iop.org/nano/26/465501/mmedia

(Some figures may appear in colour only in the online journal)

1. Introduction

Single-crystal silicon has played an important role in the evolution of micro- and nanomechanical devices. For example, nanomechanical silicon beams and membranes have been successfully used as sensors to record small forces [1] and masses [2] and led to pioneering advances in ultrasensitive scanning force microscopy [3], chemical screening [4], and biomolecular recognition [5]. Despite their small active volumes, nanomechanical devices can have very high quality factors of mechanical resonance in the range of $Q \sim 10^3$–10^7 [6, 7]. The high quality factor compared to electrical resonant circuits makes nanomechanical devices especially attractive for high-frequency signal transduction [8] and ultrasensitive, narrowband force detection [3]. Low-loss nanomechanical resonators are furthermore promising device elements for parallel data storage [9] or classical and quantum transducer architectures [10].

High quality factors are important in nanomechanical force detection, because they are intimately related to the sensitivity of a device. Through the fluctuation–dissipation theorem, the Q factor sets the amount of thermomechanical noise disturbing the sensor and thereby determines the smallest measurable force [11]. Although the force sensitivity can be limited by many other factors, such as noise in the displacement readout or instrument stability, the thermomechanical noise provides the intrinsic and fundamental limit to force measurements. High-Q resonators made from single-
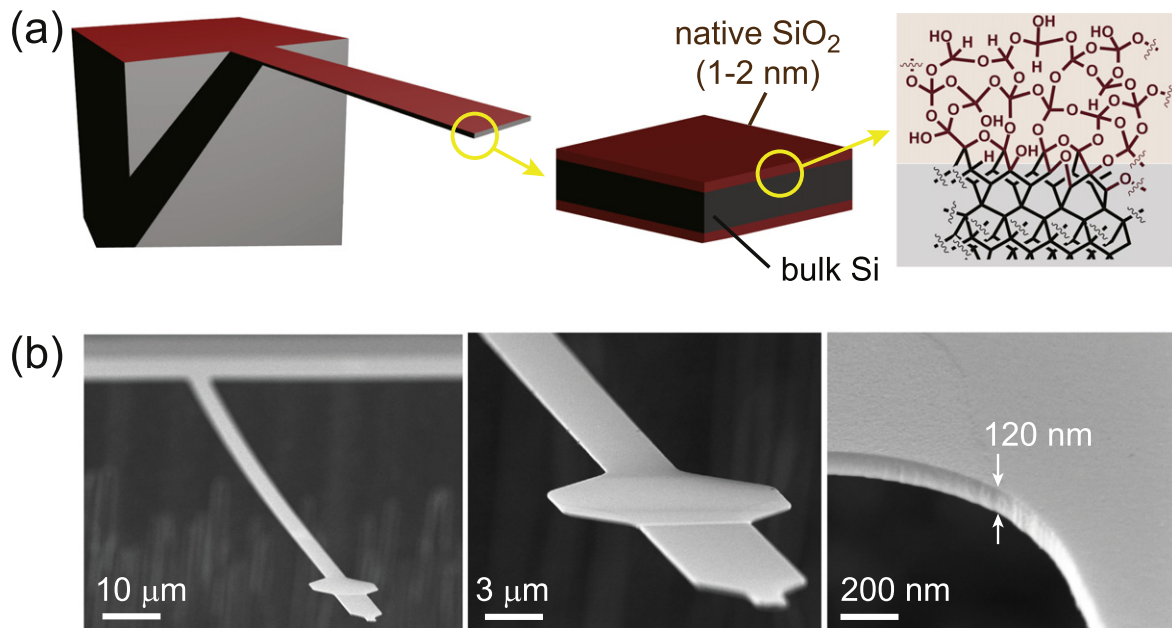
Figure 1. (a) Schematic buildup of silicon cantilever devices, showing the trimorph-like SiO_2(1 nm)–Si(120 nm)–SiO_2(1 nm) cross section and the atomistic makeup of the native surface oxide layer. Si atomic labels are omitted for clarity. (b) Scanning electron micrographs of one of the 120 nm thick cantilever devices used in this study.

crystal silicon have routinely reached this thermal noise limit and demonstrated force sensitivities of the order of 10^{-18} N (1 Attonewton) or less at cryogenic temperatures [1, 11]. Silicon has been a workhorse material for ultrasensitive nanoelectromechanical systems (NEMS) because of its low intrinsic dissipation and because it can be easily processed into a variety of shapes, including cantilevers, strings, membranes, and nanowires.

A potential drawback of silicon as a low-loss mechanical resonator material is the presence of a $\sim$1–2 nm native oxide layer on its surface [12]. The oxide layer or associated defects are believed to play a pivotal role in the mechanical friction. Even for devices as thick as several micrometers, surface-related loss has been shown to dominate mechanical friction and to lead to a linear decrease of the mechanical Q with decreasing thickness [13, 14]. The reduction in Q is particularly severe, as dimensions of devices start approaching dimensions in the deep nanometer range, such as for ultrathin silicon cantilevers [1], membranes [15], or nanowires [6, 16]. The native oxide is a complex and heterogeneous amorphous solid with a number of silicon suboxides at the bulk silicon interface and fully oxidized silicon dioxide in upper layers [17]. Oxide formation strongly depends on environmental factors such as humidity, and the precise morphology and thickness of the oxide is variable [12]. Although it is possible to remove the oxide layer by annealing to 800° C in ultra-high vacuum (UHV) [18, 19] or using chemical etching, the oxide-free silicon surface is unstable in air, and the oxide layer regrows within minutes under ambient atmosphere [12]. In a series of investigations, Henry, Hines and coworkers found that some permanent improvement in the mechanical quality factor is possible by monolayer coating of the surface with alkanes [20–22]. It is, however, unknown whether these

improvements extend to low temperatures, where many of the most sensitive measurements are carried out. Moreover, the liquid-phase chemistry is difficult to carry over to ultrasoft and fragile mechanical structures.

Here we present a detailed study of the mechanical dissipation of ultrasensitive silicon cantilevers as a function of surface termination. We show that the dissipation is proportional to the thickness of the native oxide and that it subtly depends on oxide formation conditions. We further investigate several approaches for chemical passivation of the surface, including thermal nitridation and organic monolayer deposition by liquid-phase or gas-phase hydrosilylation of medium-sized terminal alkenes, alkynes, and aldehydes. All strategies are found to achieve long-term (>1 d) protection against air oxidation and three- to five-fold quality factor improvements compared to default devices. In most cases, these improvements extend to and are even more pronounced at cryogenic temperatures. The passivation steps are procedurally simple and can be easily integrated into existing lithographic recipes and carried out with standard cleanroom equipment.

2. Experimental setup

The demonstration devices used in this study were $\langle 1, 0, 0 \rangle$-oriented cantilever beams of $\sim$120 nm thickness, 4 μm width, and lengths between 90–120 μm fabricated from an insulating single-crystal silicon substrate (see figure 1) [23]. Similar cantilevers have been extensively characterized in the context of ultrasensitive force microscopy, where they are established as some of the most sensitive nanomechanical force sensors in use [1, 3, 18, 24]. Since these cantilevers are

long and thin, thermomechanical and clamping losses are negligible [13], making them an ideal testbed to assess surface friction. Moreover, potential advances towards lower surface friction achieved in this study will directly impact pertinent force-sensing applications.

We have analyzed surface friction through measurements of the mechanical quality factor Q. The mechanical quality factor describes the energy loss per oscillation cycle, and the inverse quality factor Q^{-1} is directly proportional to the mechanical dissipation parameter, $\Gamma \propto Q^{-1}$ [13]. The quality factor Q and mechanical dissipation Γ are important parameters that directly limit the force sensitivity of a mechanical sensor [7]. For our silicon test devices, mechanical friction is composed of two different sources of friction, including the material's intrinsic (or 'bulk') dissipation Γ_0 and a surface-specific dissipation Γ_s [7, 13]. Since friction is additive, the total dissipation is given by $\Gamma = \Gamma_0 + \Gamma_s$. For most NEMS with a crystalline core, including the present silicon devices, the dominant contribution comes from the surface and $Q^{-1} \propto \Gamma_s$ [13, 14].

We have measured the mechanical Q using the ring-down method [1, 13]. Cantilevers were mounted in a custom-built atomic force microscope that allowed for mechanical excitation of devices by a small piezoelectric element. The cantilevers were briefly driven at the mechanical resonance ($f_c \sim 10$ kHz), and the ring-down of the mechanical oscillation is monitored by a low-power fiber-optic interferometer [1]. The mechanical Q is then given as $Q = \pi f_c \tau$, where τ is the $1/e$ ring-down time. All measurements were carried out in a variable-temperature cryostat (4–300 K) and in high vacuum ($p < 10^{-6}$ mbar).

For many measurements, it is important to control and minimize the time a (surface-modified) device was exposed to air. For this purpose, surface reactions were carried out in a sealed reactor chamber that could be flushed with inert gas (Ar) and transported from the wet lab to the point of measurement. Cantilevers could be mounted in the force microscope on a holder piece using a single screw, and interferometer alignment was done remotely using three-axis positioners after pump-down and in vacuum. With experience, this procedure allowed for air exposure times—defined as the interval between the first exposure of the sample to air (when opening the reaction chamber) and the start of pumping of the system—down to about 2 min. Although additional oxidation may in principle still occur after the pump is started, pump-downs were fast, and we have neglected this additional period.

3. Results and discussion

3.1. Role of native surface oxide

We initiated the study by assessing the contribution of the 1–2 nm native oxide to the total mechanical dissipation of the devices. For this purpose, we have stripped the oxide by hydrofluoric acid (HF/H_2O) vapor, resulting in an oxygen-free (hydrogen-terminated) surface. Figure 2(a) shows that the

mechanical quality factor right after ($\sim$2 min) oxide stripping increased by a factor of 6–8×, in agreement with earlier studies on UHV-annealed silicon cantilevers [19]. We found a similar increase in Q also at 4 K (see supporting information, [25]). The improvement in Q was consistent between devices from the same wafer, but a systematic difference was seen compared to a second wafer, where Q factors only improved to 40–50 K at room temperature (see supporting information).

From figure 2(a) we conclude that the native oxide layer contributes about 85% to the total dissipation in these devices. The remaining 15% is contributed by other sources, presumably residual surface damping. Although well-known mechanisms, including thermomechanical damping, clamping loss, or viscous drag [13], could in principle also be in effect, none of them is sufficiently strong to explain the $Q \lesssim 10^5$. Additional surface damping can be expected, because our devices are not atomically flat and have rough sidewalls from device lithography.

Figure 2(a) also shows that the mechanical quality factor rapidly decreased (within minutes) following air exposure due to regrowth of the native oxide. We have compared the reduction in the Q to the thickness of the oxide layer measured by x-ray photoelectron spectroscopy (XPS). XPS measurements were carried out on separate Si wafer pieces. The combined data showed a roughly linear dependence of dissipation on the thickness of regrown oxide (figure 2(b)). We conclude that the dissipation is therefore mainly generated within the oxide film and not by interfacial defects, adsorbates, or crystal termination defects [26].

We have carried out several additional experiments to better understand the mechanism of oxide formation. Figure 2(c) shows repeated cycles of hydrofluoric acid vapor cleaning followed by air exposure under different conditions. We found that the reduction in Q is reversible to within experimental error, confirming the oxide layer as the origin of dissipation and not, e.g., residual contamination during device lithography or by adsorbates. The rate of Q degradation was reduced in the dark, a result consistent with visible light-driven reactivity of hydrogen-terminated silicon surfaces [27]. We further measured no significant difference between the effects of HF and DF (deuterium fluoride) treatments, as expected from the oxide growth mechanism [28]. Finally, we observed differences in oxide growth under different atmospheres; these results are presented further below.

As an interesting side note, we found that the cyclic removal and regrowth of the native oxide layer allows us to investigate the elastic modulus (Young's modulus) and the mass density of the native SiO_2 layer. The oxide-covered silicon cantilever can be modeled as a bimorph consisting of a thick silicon layer and a thin silicon dioxide layer of twice the native oxide thickness (as both sides of the cantilever are oxide-covered). The difference Δf_c between the mechanical resonance frequencies of the bimorph ($f_c + \Delta f_c$) and the bare silicon cantilever (f_c) depends on the elastic properties of both materials as well as their thicknesses. For thin surface films
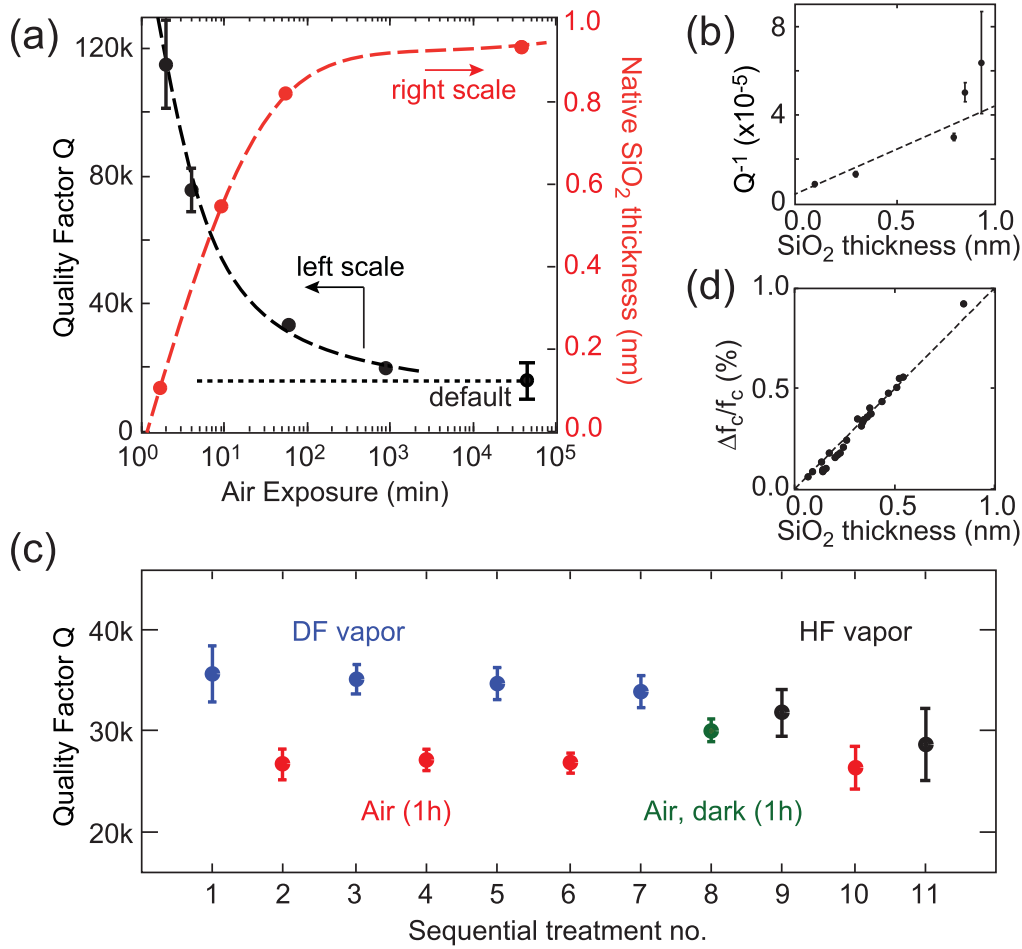
Figure 2. (a) Mechanical quality factor Q (black, left scale) and thickness of native oxide layer t_{SiO_2} measured by XPS (red, right scale) plotted as a function of ambient air exposure. Dashed lines are guides to the eye, and the dotted line is the baseline (default device with no surface oxide stripping). (b) Inverse mechanical quality factor Q^{-1} plotted against t_{SiO_2}, showing that friction increases with oxide layer thickness. Dashed line is a guide to the eye. (c) Cyclic removal and regrowth of the native oxide layer shows reversible changes in Q. Light is found to promote oxidation, while surface deuteration by DF does not influence oxide growth. The trend to lower Q with the number of removal/regrowth cycles is due to the decreasing thickness of the device. These devices were from a second wafer with generally lower Q values. (d) The fractional change in mechanical resonance frequency $\Delta f_c/f_c$ with oxide thickness t_{SiO_2} allows one to determine the Young's modulus and mass density of the surface oxide. All measurements were carried out at room temperature and under high vacuum.

$(t_{SiO_2} \ll t_{Si})$ the frequency difference is [29]

$$\frac{\Delta f_c}{f_c} = \left(\frac{3E_{SiO_2}}{2E_{Si}} - \frac{\rho_{SiO_2}}{2\rho_{Si}} \right) \frac{t_{SiO_2}}{t_{Si}}. \qquad (1)$$

Here, E_{SiO_2} and E_{Si} are the Young's moduli, ρ_{SiO_2} and ρ_{Si} the densities, and t_{SiO_2} and t_{Si} the thicknesses of the SiO_2 and Si layers. Using known parameters for bulk silicon ($E_{Si} = 171$ GPa, $\rho_{Si} = 2.329$ g cm^{-3}, $t_{Si} = 120$ nm), we can fit the linear dependence of $\Delta f_c/f_c$ on the oxide thickness t_{SiO_2} using equation (1) and obtain an estimate for either E_{SiO_2} or ρ_{SiO_2} (see figure 2(d)). Inserting the bulk value $\rho_{SiO_2} = 2.20$ g cm^{-3} [30] for the density of fused quartz, we obtain $E_{SiO_2} = 97.1 \pm 1.7$ GPa by fitting the linear dependence of $\Delta f_c/f_c$ on the oxide thickness t_{SiO_2} (see figure 2(d)). This value is larger than the commonly accepted elastic modulus of fused quartz ($E_{SiO_2,bulk} = 72$ GPa) [30, 31], which could be due to the presence of suboxides, interfacial stress, or hardening of the material by defects. The deviation could also be explained by a lower density of the native

oxide; inserting $E_{SiO_2,bulk} = 72$ GPa, we obtain a native oxide density of $\rho_{SiO_2} = 1.18 \pm 0.07$ g cm^{-3} from the fit. This density appears unrealistically low. The Young's modulus of the native oxide on the silicon surface is therefore most likely significantly higher than that of fused quartz.

3.2. Modification of surface chemistry

In order to stabilize the oxide-free surface and to maintain low mechanical dissipation for extended periods of time, we have screened various chemical surface modifications both in liquid and gas phases. The three most successful approaches are presented in figure 3 and include thermal nitridation [32] and organic monolayer deposition by liquid-phase [21] and gas-phase hydrosilylation [33].

Additional reactions tested include two-step alkylation/amination, spontaneous grafting of diazonium salt, coating of diffusion barrier layers by atomic-layer deposition and by electron beam evaporation, and a simultaneous exposure to
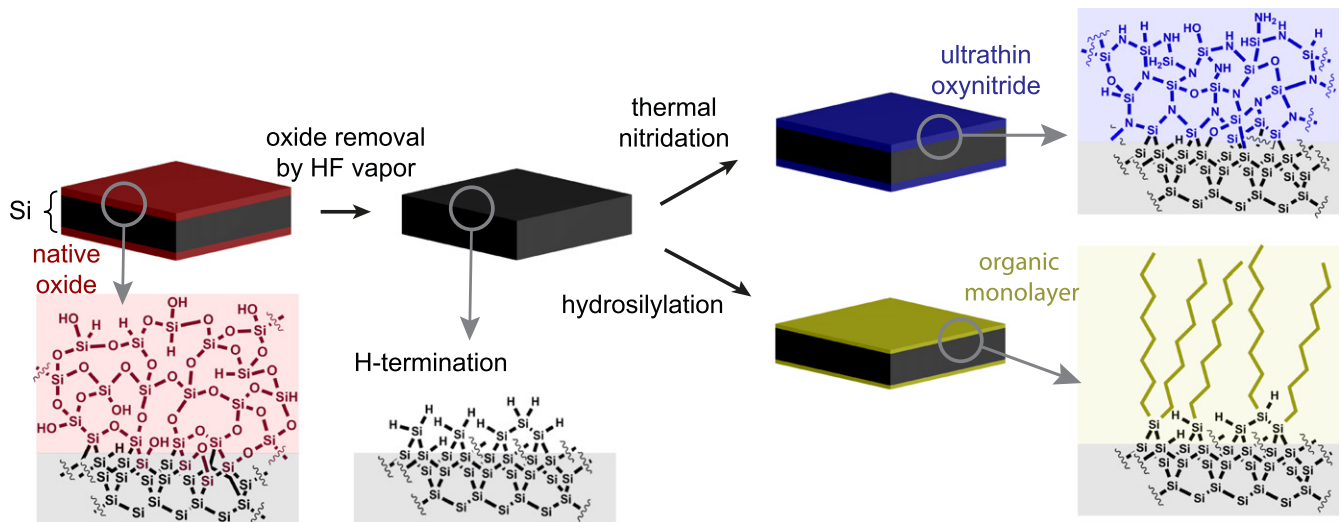
Figure 3. Schematic and atomistic pictures for chemical surface modification and passivation. In a first step, the native oxide layer (red) is removed by HF, and in a second step a surface protection reaction is carried out. Two different surface modifications are depicted, including thermal nitridation (blue) and hydrosilylation (yellow).
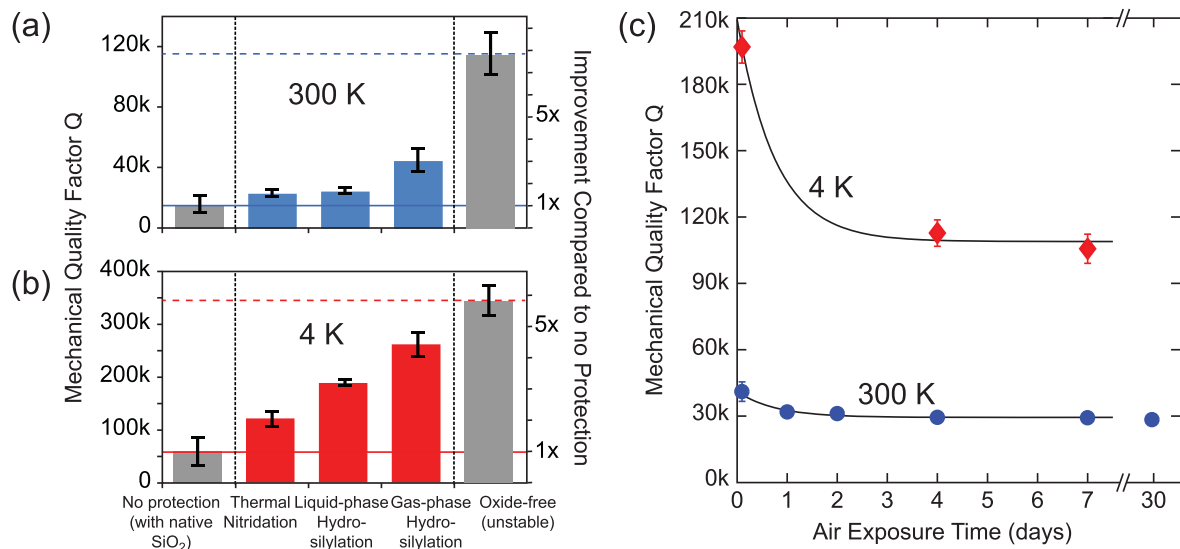

Figure 4. Long-term improvement of the mechanical quality factor Q for presented surface modifications, measured at (a) room temperature and (b) cryogenic (4 K) temperature. The first bar shows the quality factor of an untreated device and the last bar that of an oxide-stripped but unprotected device. The remaining bars show quality factors of protected devices after they were exposed to air for 24 h. The right scale shows the improvement of the quality factors relative to an untreated device. Improvements of up to 2.7× (room temperature) and 4.4× (4 K) are found for devices with an octene monolayer deposited by gas-phase hydrosilylation. (c) Quality factor of propyne-protected devices prepared by gas-phase hydrosilylation for up to one month of air exposure. A drop in quality factor is observed during day 1, possibly due to conversion of residual Si-F to Si-OH termination [33]. No further deterioration occurs thereafter. The solid line is an exponential with decay time of 1.3 days. Error bars reflect the standard deviations of between 5–46 measured devices from the same wafer and are omitted if smaller than the symbol.

HF vapor and alkenes. These results are provided as supporting information [25].

Nitridation—In a first approach, we have explored thermal nitridation as a way to passivate the surface against oxidation [32]. Although thermal nitride merely replaces one surface layer against another, one could expect that the low bulk dissipation of silicon nitride (another favorite NEMS material) will be less detrimental than lossy amorphous SiO$_2$ [25]. The thermal nitride was grown in ammonia at 700–1000 °C using a rapid thermal processing system.

Figure 4 shows that thermal nitridation has a beneficial effect, resulting in a slight (1.5×) improvement in mechanical Q at room temperature and a 2× improvement at 4 K. We found the film thickness and nitrogen content to increase significantly with reaction temperature [25], and an optimal Q was observed at 800 °C. We observed no degradation in Q after the nitride-passivated sample had been stored in ambient atmosphere for 24 h, confirming the expected long-term stability against oxidation. Overall, the silicon nitridation approach has the advantages of good air stability and
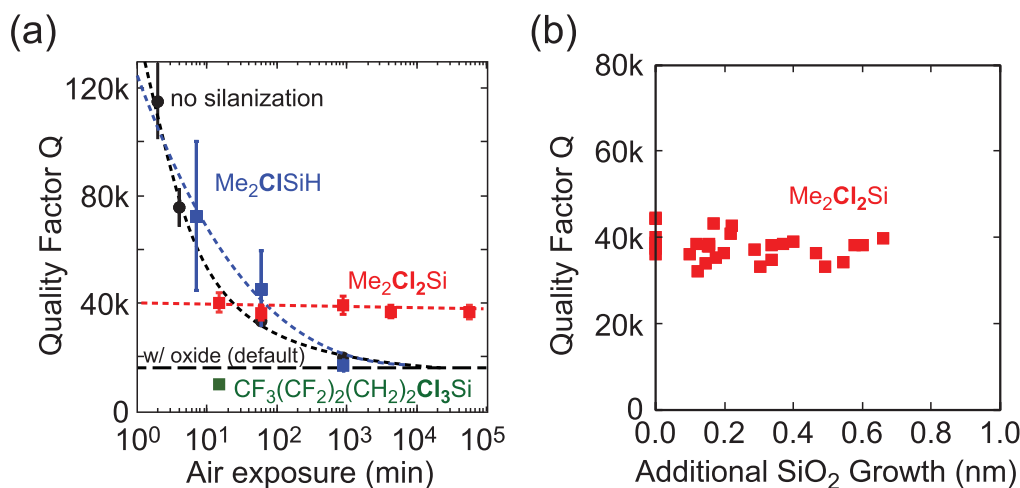
Figure 5. (a) Behavior of cantilevers that have a purposely grown oxide layer by silanization. Shown is the *Q* factor of devices that underwent silanization by mono-, di-, and trichloroalkylesilane and are then exposed to air. Almost no oxide is grown under monochloroalkylsilane atmosphere, resulting in a high initial *Q* that rapidly drops with air exposure (blue). Significant oxide is grown under dichloroalkylsilane (red) or trichloroalkylsilane (green) atmospheres, resulting in lower initial *Q* that are stable against air exposure. Curve of default device (black) is the same as in figure 2(a). (b) Native oxide continues to grow after dichloroalkylsilanization. The plot shows the mechanical *Q* as a function of the additional oxide grown (measured by XPS). Surprisingly, the *Q* factor does not change as the native oxide is formed.

operational simplicity. On the other hand, improvements in *Q* are modest (1.5–2×), and the high processing temperatures (>700° C) may not be compatible with some devices.

Liquid-phase alkylation/amination—A second approach is the formation of a self-assembled organic monolayer that blocks the access of reactive O_2 molecules. Such an approach by passes the high temperatures required for thermal nitridation and has been successfully employed for stabilizing high *Q* in doubly clamped, ⟨1, 1, 1⟩-oriented torsional oscillators [21]. We have explored three recipes for monolayer formation, including (*i*) thermal hydrosilylation of terminal alkenes and alkynes [34], (*ii*) a two-step bromination/alkylation reaction [35, 36], and (*iii*) a two-step bromination/amination process [37, 38]. The recipes had mixed success. Figure 4 shows that standard liquid-phase hydrosilylation, (*i*), enhanced the low temperature *Q* by 2–3× above the native oxide default, but we found little to no improvement at room temperature. We found minimal degradation of mechanical *Q* with time, confirming the good air stability of organic monolayers [21]. The two-step procedures (*ii*) and (*iii*), on the other hand, did not lead to improved *Q* factors [25]. In the alkylation case, (*ii*), we attribute the failure to surface contamination. For all three liquid-phase processes we found that the use of an ultraclean critical-point drying system was essential. In our study, only a brand-new instrument yielded unpolluted devices, while all other driers from shared user facilities led to devices with abysmal *Q* values due to severe cross-contamination.

Gas-phase hydrosilylation—In a third approach we have applied a simple vapor-phase thermal hydrosilylation recipe that avoids both liquid-phase and high-temperature process steps. Gas-phase hydrosilylations are not well developed in the literature, and the presented reactions were conceived to extend the hydrosilylation process to the gas phase [33]. We demonstrated the process using octene, propyne and octanal.

In contrast to the analogous liquid-phase hydrosilylation recipe, we found the gas-phase reaction to provide a significant improvement in mechanical *Q*, with 2.7× higher values at room temperature and 4.3× higher values at cryogenic temperatures. The improved performance is likely due to cleaner device surfaces in the absence of any liquid contact. Consistent with [39], chain length-matched alkene and aldehyde gave similar *Q* at room temperature. At low temperature, we found the alkyl monolayer to be slightly superior to the alkoxide monolayer.

3.3. Atomistic origin of surface dissipation

In the last part of this study we have investigated surface oxide formation under different chemical atmospheres. For this purpose, we have immersed freshly HF-cleaned devices in vapors of mono-, di-, and trichloroalkylesilane under a N_2 atmosphere for a duration of 30 min [25]. The N_2 gas had a spurious component of O_2 (roughly 0.1%), which, assisted by the silane vapors and residual moisture, led to the formation of an oxide beneath a thin alkyl layer. These oxides could then be compared to the native oxide formed in air. Not all silanes were equally efficient in promoting oxide growth, and additional oxide could still grow in air after the procedure. Reactivity increased with the number of chlorines in the silane.

As shown in figure 5(a), the oxides grown in different silanes had very different impacts on the mechanical *Q*. Monochlorodimethylsilane (Me_2ClSiH) reacted very little with the silicon surface, and the rate of *Q* deterioration was very similar to that of untreated devices. Trichloro (1H,1H,2H,2H-perfluorooctyl)silane ($CF_3(CF_2)_2(CH_2)_2Cl_3Si$), on the other hand, led to the formation of ∼2 nm of oxide beneath a fluoroalkyl monolayer [25]; the amount of oxide thus formed was thicker than the
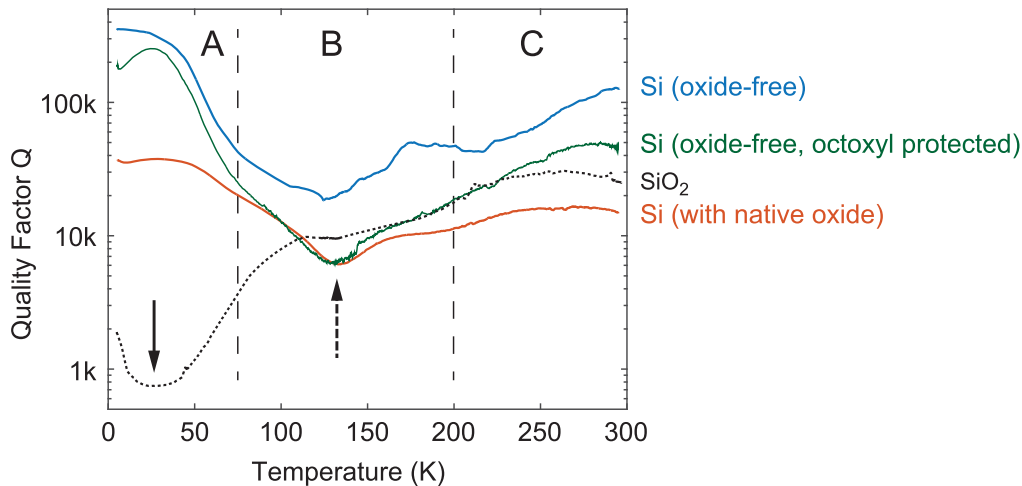
Figure 6. Quality factor as a function of temperature for three Si cantilevers (oxide-free, octoxyl-protected, native oxide) and a SiO$_2$ cantilever. A, B, and C roughly divide between regions with different sources of friction. Solid arrow indicates dissipation peak caused by SiO$_2$, and dashed arrow indicates dissipation peak possibly caused by the organic protection layer and surface adsorbates.

native oxide grown in air. Q values were slightly below those of native oxide devices.

The most interesting case is dichlorodimethylsilane (Me$_2$Cl$_2$Si), which led to an air-stable Q that was roughly $2\times$ better than that of native devices. XPS measurements revealed a thin layer of oxide beneath a polydimethylsiloxane film that continued to grow in air until the native oxide thickness (1–2 nm) was reached [25]. Despite the growth of additional oxide in air, no degradation in Q occurred. (A similar beneficial effect was found for dichlorodiethylsilane vapor, and no improvement in Q was observed if silanization occurred *after* the native oxide had already formed.) We hypothesize that the concurrent silanization/oxidation had a 'templating effect' that led to a more ordered atomic arrangement and reduced the dissipative properties of the oxide film. We more recently found that post-exposure of native oxide-bearing devices to oxygen plasma can also raise the Q factor by $2\times$ at room temperature, which may be explained by a similar (partial) rearrangement of atoms. Together, all observations support the conclusion that the amorphous nature of the native oxide, and not the simple presence of Si-O-Si bonds, is crucial to explain surface dissipation [26].

3.4. Temperature dependence of dissipation

To better understand the low-temperature improvement of the quality factor, we have compared the Q versus temperature curves for oxide-free, oxide-covered, and octoxyl-protected cantilevers (corresponding to the 1st, 4th, and 5th bar in figure 4). Two other devices with octyl and octadecyl monolayers were also prepared (see supporting information). We have further measured a curve for a fused quartz cantilever obtained by thermal oxidation of a standard Si device. Curves are presented in figure 6.

As expected, the oxide-free cantilever showed the highest Q factor of all devices over the entire temperature range. This observation can be easily understood by the absence of the native oxide layer and the organic protection layer. The

octoxyl-protected cantilever showed a Q factor that was between the oxide-free and oxide-covered cantilevers. The improvement was highest at 4 K ($\sim$5 : 1) and at 300 K ($\sim$3 : 1) and was lowest around 130 K ($\sim$1 : 1). In order to explain this behavior, it is useful to roughly divide the chart into a low-temperature region (region A in figure 6), a medium-temperature region (B), and a high-temperature region (C).

In region A (below about 70 K), the two oxide-free (protected and unprotected) cantilevers showed similar high Q values, whereas the native oxide-covered device had much lower Q. We thus suspect friction to mainly occur in the oxide layer. This hypothesis is supported by the fused quartz device, where a dramatic increase in dissipation was seen below $\sim$70 K. This increase in dissipation is attributed to tunneling two-level systems in amorphous, glass-like SiO$_2$ [40]. Considering the thicknesses of the native oxide layer ($\sim$1–2 nm) and the quartz cantilever (280 nm), the reductions in Q between the two devices even quantitatively agree. We conclude that in region A, the native oxide layer dominates friction, and the contribution by the carbonaceous surface protection is small.

In region B, at around 130 K, all Si cantilevers experience a peak in dissipation. A similar peak has been observed in many previous studies [13, 41, 42], but its origin remains unclear. Here, we believe that the organic coating and possibly a ubiquitous physisorbed molecular layer contribute the additional friction. For our devices, the organic layer was thinnest for oxide-free Si, thicker for the octoxyl-protected surface, and still thicker for the octadecyl surface (see supporting information). We observed that the thickness of the organic layer is directly correlated with the intensity of the dissipation peak in figure 6. The peak is also seen for the native oxide-covered device and for similar diamond and SiN devices (see [7] and supporting information), where it may be explained by a physisorbed molecular layer, possibly hydrocarbons [43]. The adventitious surface layer is small for all other devices, because they only experienced short air

exposure. The dissipation by the organic surface layer ceases as the temperature increases (region C) but is still partially present at 300 K.

4. Conclusions

To summarize, we have performed a detailed study of the role of the ~1–2 nm native oxide in the mechanical friction of thin (~100 nm) silicon cantilever beams. The data presented show that, for our test devices, the surface oxide contributes about 85% to the total dissipation, both at room and cryogenic temperatures. We find the friction to be proportional to the oxide thickness and to subtly depend on formation conditions, indicating that dissipation is intricately related to the atomic arrangements of the amorphous oxide. We have further developed three different chemical surface modifications, including thermal nitridation, hydrosilylation, and gas-phase silanization, that inhibit oxide formation and partially preserve the low dissipation of the oxide-free devices. The improvements in mechanical quality factor compared to default (native oxide-bearing) cantilevers are up to $3\times$ at room temperature and extend to $5\times$ at cryogenic temperatures. We suspect that even higher improvements will be seen as dimensions of nanomechanical devices continue to shrink.

We finally note that the facile surface passivation reactions may be beneficial to several technological efforts beyond the fields of micro- and nanoelectromechanical systems. The presented gas-phase reactions have several advantages over their commonly used liquid-phase counterparts, including gentle mechanical handling, scalability, and absence of cross-contamination. For instance, the surface modification of silicon nanowires may further improve the thermoelectric figure of merit (zT) of this mass-produced thermoelectric material [44, 45]. Other potential uses include surface doping in semiconductor engineering and lifetime enhancement in optoelectronic devices. Given the easy integration of presented surface modification reactions into standard cleanroom processes, the advances described may offer a simple and straightforward way to enhance a broad range of silicon nanotechnologies.

References

[1] Mamin H J and Rugar D 2001 Sub-attonewton force detection at millikelvin temperatures *Appl. Phys. Lett.* **79** 3358

[2] Ilic B, Yang Y and Craighead H G 2004 Virus detection using nanoelectromechanical devices *Appl. Phys. Lett.* **85** 2604–6

[3] Poggio M and Degen C L 2010 Force-detected nuclear magnetic resonance: recent advances and future challenges *Nanotechnology* **21** 342001

[4] Lang H P, Baller M K, Berger R, Gerber C, Gimzewski J K, Battiston F M, Fornaro P, Ramseyer J P, Meyer E and Guntherodt H J 1999 An artificial nose based on a micromechanical cantilever array *Anal. Chim.* **393** 59–65

[5] Waggoner P S and Craighead H G 2007 Micro- and nanomechanical sensors for environmental chemical and biological detection *Lab Chip* **7** 1238–55

[6] Feng X L, He R R, Yang P D and Roukes M L 2007 Very high frequency silicon nanowire electromechanical resonators *Nano Lett.* **7** 1953–9

[7] Tao Y, Boss J M, Moores B A and Degen C L 2014 Single crystal diamond nanomechanical resonators with quality factors exceeding one million *Nat. Commun.* **5** 3638

[8] Bagci T *et al* 2014 Optical detection of radio waves through a nanomechanical transducer *Nature* **507** 81–5

[9] Vettiger P *et al* 1999 Ultrahigh density high-data-rate nems-based afm data storage system *Microelectron. Eng.* **46** 11–7

[10] Poot M and Van der Zant H S J 2012 Mechanical systems in the quantum regime *Phys. Rep.–Rev. Sec. Phys. Lett.* **511** 273–335

[11] Stowe T D, Yasumura K, Kenny T W, Botkin D, Wago K and Rugar D 1997 Attonewton force detection using ultrathin silicon cantilevers *Appl. Phys. Lett.* **71** 288–90

[12] Morita M, Ohmi T, Hasegawa E, Kawakami M and Ohwada M 1990 Growth of native oxide on a silicon surface *J. Appl. Phys.* **68** 1272–81

[13] Yasumura K Y, Stowe T D, Chow E M, Pfafman T, Kenny T W, Stipe B C and Rugar D 2000 Quality factors in micron- and submicron-thick cantilevers *J. Microelectromech. Syst.* **9** 117

[14] Yang J L, Ono T and Esashi M 2002 Energy dissipation in submicrometer thick single-crystal silicon cantilevers *J. Microelectromech. Syst.* **11** 775

[15] Roberts M M, Klein L J, Savage D E, Slinker K A, Friesen M, Celler G, Eriksson M A and Lagally M G 2006 Elastically relaxed free-standing strained-silicon nanomembranes *Nat. Mater.* **5** 388–93

[16] Nichol J M, Hemesath E R, Lauhon L J and Budakian R 2008 Displacement detection of silicon nanowires by polarization-enhanced fiber-optic interferometry *Appl. Phys. Lett.* **93** 193110

[17] Seah M P *et al* 2004 Critical review of the current status of thickness measurements for ultrathin sio₂ on si part v: results of a ccqm pilot study *Surf. Interface Anal.* **36** 1269–303

[18] Mouaziz S, Boero G, Moresi G, Degen C, Lin Q, Meier B and Brugger J 2006 Combined al-protection and hf-vapor release process for ultrathin single crystal silicon cantilevers *Microelectron. Eng.* **83** 1306

[19] Rast S, Gysin U, Ruff P, Gerber C, Meyer E and Lee D W 2006 Force microscopy experiments with ultrasensitive cantilevers *Nanotechnology* **17** S189

[20] Henry J A, Wang Y and Hines M A 2004 Controlling energy dissipation and stability of micromechanical silicon resonators with self-assembled monolayers *Appl. Phys. Lett.* **84** 1765–7

[21] Henry J, Wang Y, Sengupta D and Hines M 2007 Understanding the effects of surface chemistry on q: mechanical energy dissipation in alkyl-terminated (c-1-c-18) micromechanical silicon *J. Phys. Chem. B* **111** 88–94

[22] Henry J, Wang Y and Hines M 2011 Effect of surface chemistry on the quality factors of micromechanical resonator *Proc. SPIE* **8031** 80311A

[23] Chui B W, Hishinuma Y, Budakian R, Mamin H J, Kenny T W and Rugar D 2003 Mass-loaded cantilevers with

suppressed higher-order modes for magnetic resonance force microscopy *12th Int. Conf. Solid State Sensors, Actuators and Microsystems* **2** 1120–3

[24] Rugar D, Budakian R, Mamin H J and Chui B W 2004 Single spin detection by magnetic resonance force microscopy *Nature* **430** 329

[25] See supporting information accompanying this manuscript

[26] Imboden M and Mohanty P 2014 Dissipation in nanoelectromechanical systems *Phys. Rep.* **534** 89

[27] Sun Q-Y, de Smet L C P M, van Lagen B, Wright A, Zuilhof H and Sudhölter E J R 2004 Covalently attached monolayers on hydrogen-terminated si(100): extremely mild attachment by visible light *Angew. Chem. Int. Ed.* **43** 1352–5

[28] Mascolo D, Cerofolini G F and Vlad M O 2006 A model for oxidation kinetics in air at room temperature of hydrogenterminated (100) Si *J. Appl. Phys.* **100** 054308

[29] Metcalf T H and Liu X 2013 An ultra-high Q silicon compound cantilever resonator for Young's modulus measurements *Rev. Sci. Instrum.* **84** 075001

[30] Jong B H W S D, Beerkens R G C and van Nijnatten P A 2000 Glass, 1. Fundamentals *Ullmann's Encyclopedia of Industrial Chemistry* (Weinheim: Wiley)

[31] Drane H D H *et al* 1929 Elastic constants of fused quartz. change of young's modulus with temperature *Proc. R. Soc. London Series* A **122** 274–82

[32] Hayafuji Y and Kajiwara K 1982 Nitridation of silicon and oxidized-silicon *J. Electrochem. Soc.* **129** 2102–8

[33] Tao Y manuscript in preparation

[34] Linford M R and Chidsey C E D 1993 Alkyl monolayers covalently bonded to silicon surfaces *J. Am. Chem. Soc.* **115** 12631–2

[35] Bansal A, Li X, Lauermann I, Lewis N S, Yi S I and Weinberg W H 1996 Alkylation of Si surfaces using a two-step halogenation Grignard route *J. Am. Chem. Soc.* **118** 7225–6

[36] Eves B J and Lopinski G P 2005 Formation and reactivity of high quality halogen terminated Si(111) surfaces *Surf. Sci.* **579** 89–96

[37] Bergerson W F, Mulder J A, Hsung R P and Zhu X-Y 1999 Assembly of organic molecules on silicon surfaces via the Si-n linkage *J. Am. Chem. Soc.* **121** 454–5

[38] Tian F, Taber D F and Teplyakov A V 2011 -NH- termination of the Si(111) surface by wet chemistry *J. Am. Chem. Soc.* **133** 20769–77

[39] Richter A M, Sengupta D and Hines M A 2008 Effect of surface chemistry on mechanical energy dissipation: silicon oxidation does not inherently decrease the quality factors *J. Phys. Chem.* C **112** 1473–8

[40] Mason W P and Thurston R N (ed) 1976 *Ultrasonic Properties of Glasses at Low Temperatures* vol 12 (New York: Academic)

[41] Evoy S, Olkhovets A, Sekaric L, Parpia J M, Craighead H G and Carr D W 2000 Temperature-dependent internal friction in silicon nanoelectromechanical systems *Appl. Phys. Lett.* **77** 2397

[42] Gysin U, Rast S, Ruff P, Meyer E, Lee D W, Vettiger P and Gerber C 2004 Temperature dependence of the force sensitivity of silicon cantilevers *Phys. Rev.* B **69** 045403

[43] Takahagi T, Nagai I, Ishitani A, Kuroda H and Nagasawa Y 1988 The formation of hydrogen passivated silicon single-crystal surfaces using ultraviolet cleaning and hf etching *J. Appl. Phys.* **64** 3516

[44] Hochbaum A I, Chen R, Delgado R D, Liang W, Garnett E C, Najarian M, Majumdar A and Yang P 2008 Enhanced thermoelectric performance of rough silicon nanowires *Nature* **451** 163–7

[45] Boukai A I, Bunimovich Y, Tahir-Kheli J, Yu J-K, Goddard W A III and Heath J R 2008 Silicon nanowires as efficient thermoelectric materials *Nature* **451** 168–71